■Ngày nhận bài: 10/7/2023 ■Ngày sửa bài: 15/8/2023 ■Ngày chấp nhận đăng: 26/9/2023

Compressive and electrical resistivity properties of UHPC containing different steel fibers

Đặc trưng nén và điện trở suất của bê tông cường độ siêu cao sử dụng các loại sợi thép khác nhau

> **VIET HUY LE[1,2], DUC ANH DO[1], MANH VAN NGUYEN[1], KHANH THAC NGUYEN[3], LIEM DUY NGUYEN[4*]**
[1]Department of Civil engineering, Hanoi University of Mining and Geology
[2]Geotechnical Engineering, Construction Materials and Sustainability Research group, Hanoi University of Mining and Geology
[3]Department of Electromechanical, Hanoi University of Mining and Geology
[4]Faculty of Civil Engineering, Ho Chi Minh City University of Technology and Education,
*Corresponding author: E-mail: liemnd@hcmute.edu.vn

ABSTRACT
This study is focused on investigating the self-sensing characteristices of smart UHPCs through evaluating the mechanical and electrical properties of ultra-high-performance concretes (UHPCs) containing different steel fiber types as functional fillers under compression. UHPCs containing 2 vol% stainless smooth fibers (6 mm in length and 0.2 mm in diameter, FL6) or 2 vol% brass coated smooth fibers (13 mm in length and 0.2 mm in diameter, FL13) or 2 vol% hybrid of FL6 and FL13 were prepared and evaluated. The test results indicated that The UHPC containing FL13 produced the highest compressive strength and the lowest electrical resistivity. The flowability and the volume weight of UHPCs were little influenced by fiber types. The UHPC with hybrid of FL6 and FL13 produced the highest fractional change in electrical resistivity (FCR) under compression. Besides, the correlation between FCR and compressive stress of UHPCs was obtained.
Keywords: Electrical resistivity; self sensing; steel fiber; structural health mornitoring; ultra high performance concrete.

TÓM TẮT
Bài báo tập trung nghiên cứu các đặc trưng tự cảm biến của bê tông thông minh cường độ siêu cao sử dụng các loại sợi thép như chất tăng cường độ dẫn điện thông qua đánh giá đặc trưng cơ học và điện trở suất dưới tác dụng của tải trọng nén. Vật liệu UHPC chứa 2% thể tích sợi thép trơn không gỉ (dài 6 mm và đường kính 0,2 mm, FL6) hoặc chứa 2% thể tích sợi trơn được phủ đồng (dài 13 mm và đường kính 0,2 mm, FL13) hoặc hỗn hợp 2% thể tích của FL6 và FL13 đã được chuẩn bị và đánh giá. Kết quả thí nghiệm chỉ ra rằng UHPC chứa FL13 tạo ra cường độ chịu nén cao nhất và điện trở suất thấp nhất. Khả năng chảy và trọng lượng thể tích của UHPC ít bị ảnh hưởng bởi sử dụng các loại sợi thép khác nhau. UHPC với sự kết hợp giữa FL6 và FL13 tạo ra sự thay đổi lớn nhất về điện trở suất (FCR) khi nén. Bên cạnh đó, mối tương quan giữa FCR và ứng suất nén của các loại UHPC đã được thiết lập trong nghiên cứu.
Từ khóa: Điện trở suất; tự cảm biến; sợi thép; giám sát sức khỏe kết cấu; bê tông cường độ siêu cao.

1. INTRODUCTION

Structural-health-monitoring (SHM) system for infrastructures has been an interesting topic. It is applied to important infrastructures to prevent the sudden deterioration of infrastructures which can cause human casualties and property damages. Current sensors such as strain gauges, fiber bragg grating sensors, piezo-ceramic transducers, fiber optical sensors, and lead zirconate titanate sensors are generally utilized in the SHM. However, the limitations of these sensors are high cost, low durability, and localized sensing ability.

Smart concretes with self-sensing abilities (self-damage and self-stress sensing) recently have been developed to SHM systems of infrastructures [1]. They can overcome the drawbacks of commercial sensors used for SHM. The self-sensing of smart concretes is ability to observe the crack/damage or stress/strain of structures based on the change in their electrical resistance under external loads owing to change in their conductive network. Smart concretes can be developed by adding electrically conductive materials (functional fillers) to improve the conductive network. The functional fillers generally used in smart concretes include carbon nanotubes (CNTs), multi-wall carbon nanotubes (MWCNTs), carbon black, carbon fibers, steel fibers, nickel, graphene, or hybrid materials [2-9].

However, the self-stress sensing ability of smart concretes has been limited until 20 MPa [10] because of the low strength of concretes. To improve self-stress sensing ability of smart concrete, the self-stress sensing of ultra high-performance concrete (UHPC) should be developed. However, the reports of the self-stress sensing of ultra high-performance concrete have been still limited because of difficult distribution of functional fillers in the high density microstructure of UHPCs and low water per cement ratio. Recently, Lee et al. and Le et al. [10,11] used steel slag aggregates and short steel fibers as functional fillers in smart UHPCs for improving the compressive stress sensing ability. Le et al. [12] investigated the self-damage sensing ability of smart UHPCs using short smooth steel fibers as a functional filler. Nguyen et al. [13] investigated the self-damage sensing ability of high performance concretes using carbon black and ground granunated blast furnace slag. However, the self-stress sensing ability as well as the mechanical properties of smart UHPC using hybrid conductive short steel fibers have not been investigated.

In this study, we aim to clearly find effect of adding hybrid conductive short steel fibers on the mechanical properties as well as the electrical resistivity of UHPC under compression. The characteristics of UHPC matrices containing hybrid of 1 vol% short smooth stainless steel fiber and 1 vol% brass coated steel fibers were compared to UHPCs containing 2 vol% short smooth stainless steel fibers (6 mm in length) and UHPC containing 2 vol% brass coated steel fibers (13 mm in length). The results of UHPC containing 2 vol% smooth stainless steel fibers (6 mm in length) were adopted from [14].

2. THE ELECTRICAL RESISTIVITY CHARACTERISTICS OF SMART CONCRETES

The self-sensing ability of smart concretes is evaluated through the initial electrical resistivity (ρ_o) or resistance (R_o) and the fractional change in electrical resistivity (FCR) under external loads. The electrical resistivity (ρ) of the smart concretes is calculated based on the measured electrical resistance (R) obtained from alternative current (AC) [10,12] or direct current (DC) [9,11] measurements using Eq. (1).

$$\rho = R\frac{A}{L} \quad (1)$$

where L is the distance between two probes and A is the cross section area of sample.

The electrical conductive network of smart concretes containing functional fillers includes three main conductive paths (the ionic conduction, the contacting conduction, and the tunneling conduction). The ionic conduction is based on the movement of ions (K+, Na+, OH-) in continuous pore systems [1]. The contacting conduction is the result of the movement of free electrons in the contacting conductive path of functional fillers [1]. The tunneling conduction occurs when electrons can jump through the energy barriers between the fillers (the distance between the fillers is small enough) in a composite [1].

The AC measurement was generally preferred to avoid the polarization effects and electrode-matrix contacting effects [14,15]. Two probes and four probes which were made from highly electrically conductive electrodes such as steel fibers, copper plate, copper wire mesh, copper tape, and silver paint were utilized for AC or DC measurements. In case of DC measurement, the initial electrical resistance measured by two probes method is normally higher than that by four probes method owing to effect of contacting resistance between electrodes and matrices [1]. However, the measurement with two probes is more simple to setup and the fractional change in the electrical resistance still can clearly observed under external load. Two probes were generally incorporated with the AC measurement method to evaluate the self-sensing ability of smart concretes.

Under external load, the distance between FFs or the number of connection between FFs changed and resulted in the change in the conductive network into smart concretes, i.e., the electrical resistivity of smart concretes changed [1,6,10]. Thus, based on the fractional change in the electrical resistivity (FCR) of smart concretes, the stress or strain of smart concretes would be observed. In addition, a generation of crack also changed the conductive network inside smart concretes and would be detected based on the change in the electrical resistivity [12]. The self- sensing abilities of smart concretes were evaluated by calculating the fractional change in electrical resistivity at the peak stress (FCR) according to Eq. (2),

$$FCR = (\rho_p - \rho_o)/\rho_o \quad (2)$$

which ρ_p is the electrical resistivity of the composites at the maximum compressive stress.

3.1. Materials and specimen preparation

Table 1 summarizes the matrix components of UHPCs by weight ratios. Three UHPC matrices include UHPC containing 2 vol% short smooth stainless steel fibers (F2L6), UHPC containing 2 vol% brass coated steel fibers (F2L13), and UHPC containing hybrid of 1 vol% stainless steel fibers and 1 vol% brass coated steel fibers (F2L6L13). Cement Type I according to ASTM standard was used. Average diameter of silica sand is around 0.2 mm while that of silica fume and silica powder are around 10 µm and 100 µm, respectively. Water per cement ratio (W/C) by weight was 0.2 and the volume content of steel fibers was 2 vol%. Fig. 1 shows the images of short smooth strainght steel fibers (2104 MPa in tensile strength and 200 GPa in elastic modulus).

Table 1. Composition of matrix by weight ratio

Notation	C	SF	SPD	SS	W	SP	F vol%	
							FL6	FL13
F2L6	1	0.15	0.3	1.0	0.2	0.042	2.0	
F2L13	1	0.15	0.3	1.0	0.2	0.042	-	2.0
F2L6L13	1	0.15	0.3	1.0	0.2	0.042	1.0	1.0

C: cement, SF: silica fume, SPD: silica powder, SS: silica sand, W: water, SP: superplasticizer, F vol%: fiber volume content, FL6 and FL13: fibers with 6 and 13 mm in length, respectively.

Cubic specimens (50 x 50 x 50 mm^3) containing two embedded copper wire meshes were prepared to measure the electrical resistivity response of smart UHPCs under compression while those with no embedded meshes were used to evaluate the compressive strength of UHPCs under compression.

A Hobart-type mixer (20 *l* capacity) was utilized to prepare specimens. The sand, silica fume, cement, and silica powder were first dry-mixed for 5 min. Water was then added and further mixed for 5 min. Super-plasticizer was slowly added and the mixture was continuously mixed for approximately 3 min. The flow of mixtures was measured prior to adding fibers using mini flow cone table test. When the mixtures showed a suitable workability for a uniform fiber distribution, the short smooth fibers were manually dispersed and the mixture containing the fibers was further mixed for 1 min. The flow values of the UHPCs is listed in Table 1.

The UHPC mixtures with fibers were poured into cubic molds. Copper wire meshes (45 mm and 70 mm in width and height, respectively) were embedded in the specimens as electrodes for measuring their electrical resistivity. The distance between the two copper wire meshes was 20 mm. Specimens were slightly vibrated to reduce voids in matrices and enhance contact between wire meshes and matrices. All specimens were stored at room temperature (20 ± 2 °C) and covered with plastic sheets for 48h before demolding. Then, they were cured in a hot water tank at 90 °C for 72h and continuously stored in Laboratory zoom until testing day.

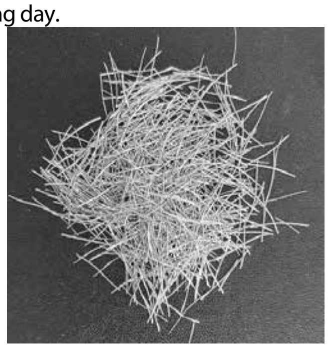

a) Stainless steel fibers 6 mm in length (FL6)

b) Brass coated steel fibers 13 mm in length (FL13)

Figure 1. Images of short smooth steel fibers

3.2. Test set-up

The flowability of fresh UHPCs were tested using a mini cone as shown in Fig. 2. The flow value was average of two diameter flow values measured according to two perticular directions. Fig. 3 displays the experimental set-up for determining the compressive stress and the electrical resistivity response of UHPC specimens during compressive testing. The compressive load was performed using a universal testing machine (UTM) with capacity of 300 tf while the electrical resistance was measured using the SI 1260 impedance/gain-phase analyzer machine. The loading speed of the UTM was maintained as 1.0 mm/min during testing. The history of the electrical resistance of specimens during tests was measured using the two probes AC measurement method with a fixed frequency of 100 Hz [10]. At least three specimens from each series were tested. The electrical resistivity of UHPCs was determined according to Eq. (1).

a) Mini cone

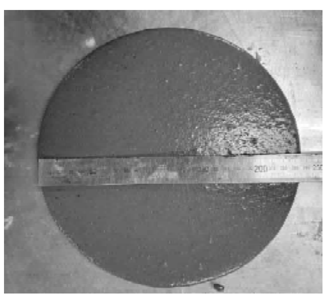

b) Flow measurement

Figure 2. Flow test using mini cone

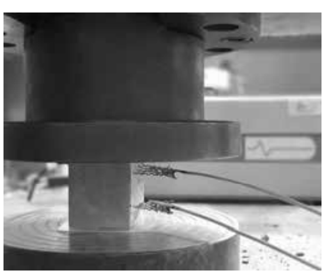

Figure 3. Test set-up for measuring the compressive stress and electrical resistance of UHPCs

4. RESULTS AND DISCUSSIONS

4.1. Flow, weight, and compressive strength of UHPCs

As summarized in Table 2, the flowability of UHPCs was almost not influenced by adding a low fiber volume content (2 vol%) regardless of fiber types or hybrid of them. The flow of smart UHPCs was 240 mm for all matrices. Darssini et al. [15,16] also reported that short fibers with low volume did not affect the concrete workability as much as the long fibers.

The volume weight values of F2L6, F2L13, and F2L6L13 were 2472.3, 2478.2, and 2487.3 kg/m^3. The volume weight of UHPC matrices was a little different because of the same volume content and weight of fibers.

Table 3 summarized the compressive strength values of UHPCs with different fibers types. The UHPC matrices with longer fibers (13 mm in length) produced higher compressive strength than that of the UHPC with shorter fibers (6 mm in length). The longer fibers with brass-coated steel provided a higher bond between fiber and matrix and resulted in increasing the crack resistance for matrices [17]. Thus, the compressive strength of UHPC matrices with longer fibers would be improved. [18] also obtained a higher compressive strength of a high performance concretes containing longer fibers in comparison with shorter fibers.

Table 2. Flow, weight, and compressive strength of UHPCs

Notation	Flow (mm)	Weight (kg/m^3)	Compressive strength (σ_p) (MPa)
F2L6	240	2472.3 (9.6)	172.5 (1.9)
F2L13	240	2478.2 (5.8)	193.6 (3.3)
F2L6L13	240	2487.3 (3.6)	173.7 (3.4)

The value in brackets is the standard deviation.

Table 3. Self-sensing characteristics of UHPCs under compression

Test series	ρ_o (kΩ.cm)	$\Delta\rho$ (kΩ.cm)	*FCR (%)*
F2L6	764.0 (28.6)	157.4 (10.9)	20.5 (0.7)
F2L13	514.0 (12.8)	131.8 (14.0)	25.6 (2.4)
F2L6L13	659.1 (34.3)	174.5 (3.3)	26.6 (1.8)

The value in brackets is the standard deviation.

a) F2L6

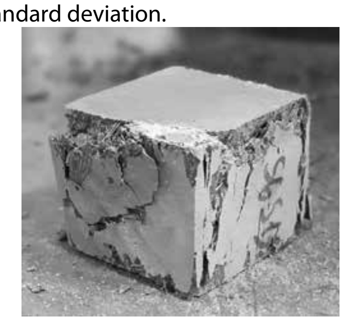

b) F2L6L13

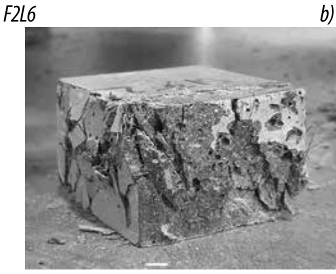

c) F2L13

Figure 4. Fracture images of UHPC specimens

4.2. Electrical resistivity properties of smart UHPCs under compression

The utilization of longer fibers (13 mm in length) produced a lower electrical resistivity of UHPC matrix with 6 mm in length fibers. The electrical resistivity of F2L6, F2L13, and F2L6L13 was 764.0 kΩ.cm, 514.0 kΩ.cm, and 659.1 kΩ.cm, respectively. In gauge length of measurement by around 20 mm, longer fibers (13 mm in length) would generate a better conductive pathway. In addition, brass-coated fibers generated higher electrical conductivity than stainless-steel fibers and consequently produced a lower electrical resistivity.

Fig. 5 shows the electrical resistivity responses of the UHPCs containing short smooth steel fibers under compression. In general, the electrical resistivity response of the UHPCs under compression can devide into three stages as follows: (1) the electrical resistivity significantly decreased as the stress increased from 0 to maximum stress (σ_{max}); (2) after the peak stress, as the compressive stress decreased, the electrical resistivity continuously decreased until a minimum value; and (3) as the compressive stress continuously decreased, the electrical resistivity was almost stable or slightly increased. In the first stage, as the compressive stress increased prior to the peak stress, the compressive strain increased and the distance between adjacent steel fibers decreased while the number of their connection increased. Thus, the contacting conduction of the composite increased and consequently its electrical conductivity increased. In the second stage, the electrical resistivity continuously decreased even after peak stress because of fibers bridging crack. During crack opening, as the compressive strain continuously increased, steel fibers were contacted at the crack position. Thus, the electrical conductivity of the UHPCs continuously increased even matrix cracking. In the third stage, the electrical conductive pathways of conductive fibers were well formed, thus the conductivity of the composite would be stable when the macro-cracks continuously were generated. The electrical resistivity in the third stage slightly increased because of opening macro-cracks. During crack opening, fibers were pulled out and resulted in gradually increasing the electrical resistivity.

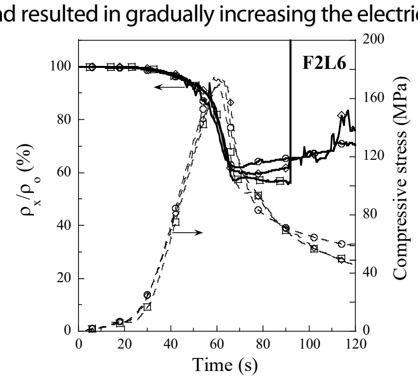

a) F2L6 [14]

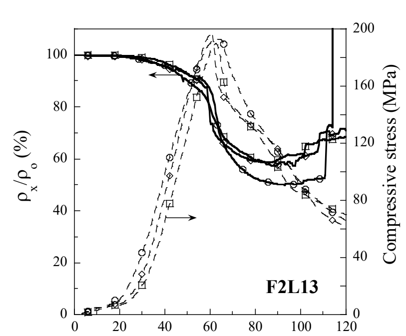

b)F2L13

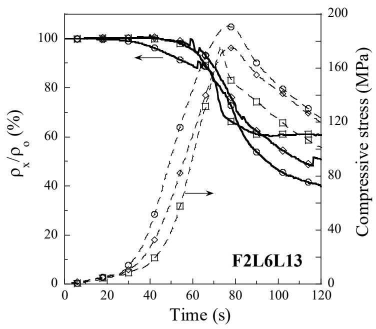

c)F2L6L13

Figure 5. The electrical resistivity response of smart UHPCs under compression

The UHPC matrix with a combination of both 6 and 13 mm in length fibers produced better FCR. As the compressive strain at the maximum compressive stress was significant, the conductive network of F2L6L13 with a combination of both 6 and 13 mm in length produced a better response and consequently generated a higher FCR.

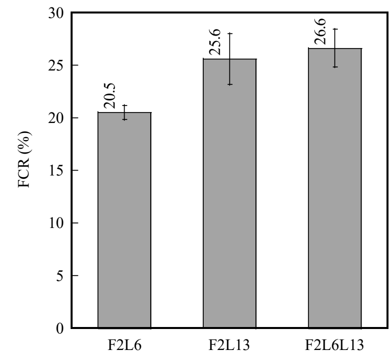

Figure 6. FCR of UHPC matrices with different fiber types at σ_p

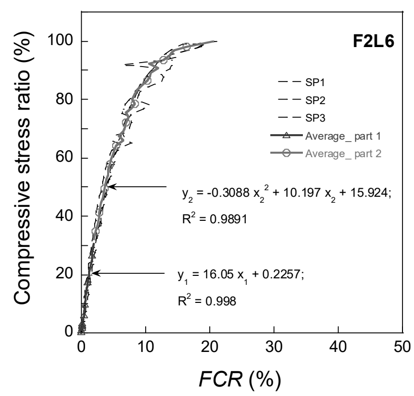

a) F2L6 [14]

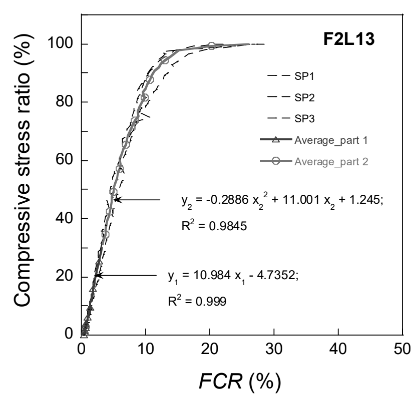

b) F2L13

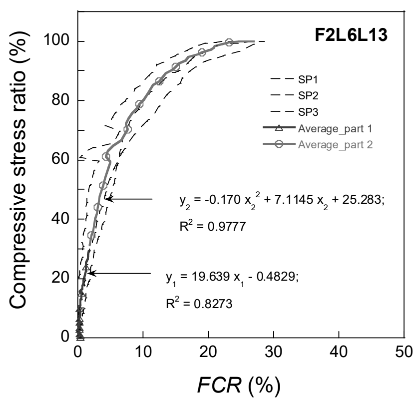

c) F2L6L13

Figure 7. Correlation between the compressive stress ratio and FCR of UHPCs

Fig. 7 presents the correlation between the compressive stress ratio (σ/σ_p) and the FCR of smart UHPC matrices and fitting equations as follows:

Part 1: σ/σ_p = a FCR + b when $0 \le \sigma \le 0.3\sigma_p$

Part 2: σ/σ_p = c FCR^2 + d FCR + e when $0.3\sigma_p < \sigma \le \sigma_p$(3)

In part 1, as the compressive stress increased from 0 to $0.3\sigma_{max}$, the composite worked in the elastic region [1,11], and the compressive stress linearly increased with increasing compressive strain [1]. In this stage, as the compressive strain increased, the distance between FFs increased and consequently the electrical resistivity linearly decreased. In part 2, generation of cracks into composites resulted in a reconstruction of the conductive network in the matrices. Thus, in part 2 the electrical resistivity non-linearly decreased. The correlation between the σ/σ_p and FCR in this part was fitted by a parabolic curve. Fitting values are shown in Fig. 7.

5. CONCLUSIONS

This experimental study investigated the effects of different types of steel fibers and their hybrid on the mechanical and the electrical resistivity properties of UHPCs under compression. Some conclusions are drawn as following:

• The flowability of fresh UHPCs was almost not influenced by adding 2 vol% steel fibers, regardless of fiber type. The volume weight of UHPCs was also little influenced by fiber types.

• The compressive strength of UHPC containing brass coated steel fibers (13 mm in length, FL13) was higher than that of UHPC containing FL6 or hybrid of FL13 and FL6.

• The electrical resistivity of UHPC containing FL13 produced a lower value than that of UHPC containing FL6 or hybrid of FL13 and FL6.

• The addition of a hybrid of FL13 and FL6 provided a better self-sensing ability (FCR) of UHPCs owing to better conductive network than adding single type of FL13 or FL6.

• A correlation between FCR and compressive stress of different UHPCs with different fiber types was obtained. The compressive stress can be determined based on the FCR of UHPCs under compression or versus.

6. ACKNOWLEDGEMENT

Authors thank the Education and Training Ministry for financial support from Project B2022-MDA-05. In addition, authors thank the testing equipment support of the ACCL Lab at Sejong University.

REFERENCES

[1] B. Han, X. Yu, J. Ou, Self-sensing concrete in smart structures, Butterworth Heinemann, Elsevier, Kidlington, 2014. https://doi.org/10.1016/C2013-0-14456-X.

[2] D.L. Nguyen, D.J. Kim, D.K. Thai, Enhancing damage-sensing capacity of strain-hardening macro-steel fiber-reinforced concrete by adding low amount of discrete carbons, Materials (Basel). 16 (2019). https://doi.org/10.3390/ma12060938.

[3] A. Downey, A. D'Alessandro, M. Baquera, E. García-Macías, D. Rolfes, F. Ubertini, S. Laflamme, R. Castro-Triguero, Damage detection, localization and quantification in conductive smart concrete structures using a resistor mesh model, Eng. Struct. 148 (2017) 924-935. https://doi.org/10.1016/j.engstruct.2017.07.022.

[4] R. Siddique, A. Mehta, Effect of carbon nanotubes on properties of cement mortars, Constr. Build. Mater. 50 (2014) 116-129. https://doi.org/10.1016/j.conbuildmat.2013.09.019.

[5] Y. Wang, L. Zhang, Development of self-sensing cementitious composite incorporating hybrid graphene nanoplates and carbon nanotubes for structural health monitoring, Sensors Actuators A Phys. 336 (2022) 113367. https://doi.org/10.1016/j.sna.2022.113367.

[6] H.V. Le, M.K. Kim, S.U. Kim, S.-Y. Chung, D.J. Kim, Enhancing self-stress sensing ability of smart ultra-high performance concretes under compression by using nano functional fillers, J. Build. Eng. 44 (2021) 102717. https://doi.org/10.1016/j.jobe.2021.102717.

[7] B. Han, K. Zhang, X. Yu, E. Kwon, J. Ou, Nickel particle-based self-sensing pavement for vehicle detection, Measurement. 44 (2011) 1645-1650. https://doi.org/10.1016/j.measurement.2011.06.014.

[8] D.D.L. Chung, Self-monitoring structural materials, Mater. Sci. Eng. R Reports. 22 (1998) 57-78. https://doi.org/10.1016/S0927-796X(97)00021-1.

[9] B. Han, J. Ou, Embedded piezoresistive cement-based stress/strain sensor, Sensors Actuators, A Phys. 138 (2007) 294-298. https://doi.org/10.1016/j.sna.2007.05.011.

[10] S.Y. Lee, H.V. Le, D.J. Kim, Self-stress sensing smart concrete containing fine steel slag aggregates and steel fibers under high compressive stress, Constr. Build. Mater. 220 (2019) 149-160. https://doi.org/10.1016/j.conbuildmat.2019.05.197.

[11] H.V. Le, D.H. Lee, D.J. Kim, Effects of steel slag aggregate size and content on piezoresistive responses of smart ultra-high-performance fiber-reinforced concretes, Sensors Actuators, A Phys. 305 (2020) 111925. https://doi.org/10.1016/j.sna.2020.111925.

[12] H.V. Le, D.J. Kim, Detecting crack and damage location in self-sensing fiber reinforced cementitious composites, Constr. Build. Mater. 240 (2020) 117973. https://doi.org/10.1016/j.conbuildmat.2019.117973.

[13] D.L. Nguyen, V.T.B. Nga, D.X. Son, M.P. Tran, Nghiên cứu dùng muội than đen và xỉ lò cao nghiền mịn trong việc cải thiện khả năng tự cảm biến của bê tông tính năng cao, Tạp chí Khoa học công nghệ xây dựng NUCE. 13 (2019) 151-158.

[14] L.H. Viet, L. Dao Phuc, N.T. Thuong, N.T. Thanh, D.L. Nguyen, D.J. Kim, Improvement of the stress sensing ability of ultra-high-performance concrete using short steel fibers and steel slag aggregates under high compression, Sensors Actuators A. Phys. 362 (2023) 114616. https://doi.org/10.1016/j.sna.2023.114616.

[15] D. Ravichandran, P.R. Prem, S.K. Kaliyavaradhan, P.S. Ambily, Influence of fibers on fresh and hardened properties of Ultra High Performance Concrete (UHPC)-A review, J. Build. Eng. 57 (2022) 104922. https://doi.org/10.1016/j.jobe.2022.104922.

[16] J. Gong, Y. Ma, J. Fu, J. Hu, X. Ouyang, Z. Zhang, H. Wang, Utilization of fibers in ultra-high performance concrete: A review, Compos. Part B Eng. 241 (2022) 109995. https://doi.org/10.1016/j.compositesb.2022.109995.

[17] D.L. Nguyen, J. Song, C. Manathamsombat, D.J. Kim, Comparative electromechanical damage-sensing behaviors of six strain-hardening steel fiber-reinforced cementitious composites under direct tension, Compos. Part B Eng. 69 (2014) 159-168. https://doi.org/10.1016/j.compositesb.2014.09.037.

[18] N.D. Liêm;, T.M. Tiến;, T.N. Thanh; Đ.X. Sơn, Đánh giá khả năng hấp thụ năng lượng của bê tông tính năng cao dưới tải trọng nén và uốn, Xây dựng. (2022) 110-114.